

## Self-affinity in the gradient percolation problem

Alex Hansen,<sup>\*</sup> G. George Batrouni,<sup>†</sup> and Thomas Ramstad<sup>‡</sup>

*Department of Physics, Norwegian University of Science and Technology, N-7491 Trondheim, Norway*

Jean Schmittbuhl<sup>§</sup>

*Institut de Physique du Globe de Strasbourg, UMR CNRS 7516, 5, rue René Descartes, F-67084 Strasbourg, France*

(Received 22 November 2005; revised manuscript received 15 December 2006)

We study the scaling properties of the solid-on-solid front of the infinite cluster in two-dimensional gradient percolation. We show that such an object is self-affine with a Hurst exponent equal to  $2/3$  up to a cutoff length  $\sim g^{-4/7}$ , where  $g$  is the gradient. Beyond this length scale, the front position has the character of uncorrelated noise. Importantly, the self-affine behavior is robust even after removing local jumps of the front. The previously observed multifractality is due to the dominance of overhangs at small distances in the structure function. This is a crossover effect.

DOI: XXXX

PACS number(s): 64.60.Ak, 02.50.-r, 05.40.Fb

Rough surfaces showing nontrivial scaling properties have been extensively studied theoretically, numerically, and experimentally over the last couple of decades. Examples of such surfaces are those appearing during brittle fracture [1], which were first characterized as being fractal [2] but it was then realized that the concept of self-affinity was more appropriate [3]. The question of self-affinity versus fractality has also been the focus of intense research on invasion fronts in porous media and on the dynamics of magnetic domain walls [4]. It was recently reported that the displacement fronts in self-affine fractures are self-affine [5]. More recently, a possible explanation for the observed self-affinity of fracture surfaces has been proposed and hinges on a clear understanding of the distinction between fractality and self-affinity [6,7]. It has also been suggested that brittle fracture surfaces are multifractal rather than simply self-affine [8]. Whether this is so remains an open question [9].

It is the aim of this Rapid Communication to study the question of fractality, self-affinity, and multifractality of a front in a system, which is simple enough to be tractable, namely, that of the gradient percolation [10]. In the literature there are already studies of this system in the present context. Furberg *et al.* [11] study the jumps in the position of the solid-on-solid (SOS) front of the infinite cluster, whereas Asikainen *et al.* [12] conclude that this front is multifractal. We will show that in this Rapid Communication up to a given scale, the SOS front is *self-affine* with a well-defined Hurst exponent, whereas on larger scales its position becomes uncorrelated. The self-affinity is *not* caused by the jumps in the position of the front due to overhangs, but is related to its fractal structure. The multifractality seen by Asikainen *et al.* has its origin in the overhangs resulting from the definition of the SOS fronts and shows up in the structure function on small scales.

In *gradient* percolation, a spatial gradient in the occupation probability  $p$  is introduced. A Cartesian coordinate system  $(i, j)$  is oriented with respect to the finite lattice of size  $L_i \times L_j$  (assuming for the rest of this paper that the lattice is two dimensional), so that the  $i$  axis runs perpendicular to the gradient (i.e., along the lower edge) and the  $j$  axis along the gradient (i.e., the left edge). The gradient is introduced in the  $j$  direction so that  $p(j) = gj$ , where the gradient  $g = 1/L_j$ . However, the cluster connected to the lower edge will reach some average value  $j = j_g$ , with an associated occupation probability  $p_g = gj_g$ . The region around  $j_g$  is critical and has a width  $\xi$ , spanning between  $j_{\pm} = j_g \pm \xi/2$ , where  $\xi$  is the correlation length associated with the critical region in the direction of the gradient. Defining  $p_{\pm} = gj_{\pm}$  and setting  $\xi = |p_{\pm} - p_g|^{-\nu} = |g(j_{\pm} - j_g)|^{-\nu}$ , where  $\nu$  is the correlation length exponent, Sapoval *et al.* [10] found that  $\xi \sim g^{-\nu/(1+\nu)} = g^{-4/7}$ .

The infinite cluster has a fractal structure with an upper cutoff in length scale set by the width of the critical region  $\xi$ . We now focus on the front of this infinite cluster and define precisely what we mean by this front  $j(i)$  in the gradient percolation problem. Our starting point is the perimeter of the cluster of occupied sites that is attached to the  $p=1$  edge of the lattice. Since this perimeter contains overhangs and therefore is multivalued when interpreted as a function  $j(i)$ , we use the SOS method to extract a single-valued function for its position (see Fig. 1). For each  $i$ , we use either the  $j$  value, which is closest to the  $p=0$  edge (top side) or the  $j$  value, which is closest to the  $p=1$  side (bottom side) or the average over all the  $j$  values attached to a given  $i$  value (average front).

A trace  $j(i)$  is statistically self-affine if the probability density  $\pi(i, j)$ , for it to have a value  $j$  at  $i$ , given that  $j=0$  at  $i=0$ , has the invariance

$$\lambda^{\zeta} \pi(\lambda i, \lambda^{\zeta} j) = \pi(i, j), \quad (1)$$

where  $\zeta$  is the Hurst exponent. This invariance must be caused by *spatial correlations* in  $j$  along the  $i$  axis. We note that a Lévy flight, which is an uncorrelated random walk whose step size  $h$  is drawn from a power-law distribution  $N(h) \sim h^{-\beta-1}$ , will satisfy Eq. (1) with an apparent Hurst ex-

<sup>\*</sup>Electronic address: Alex.Hansen@phys.ntnu.no

<sup>†</sup>Present address: INLN, UMR CNRS 6618, Université de Nice-Sophia Antipolis, 1361 route des Lucioles, F-06560 Valbonne, France; electronic address: George.Batrouni@inln.cnrs.fr

<sup>‡</sup>Electronic address: Thomas.Ramstad@phys.ntnu.no

<sup>§</sup>Electronic address: Jean.Schmittbuhl@eost.u-strasbg.fr

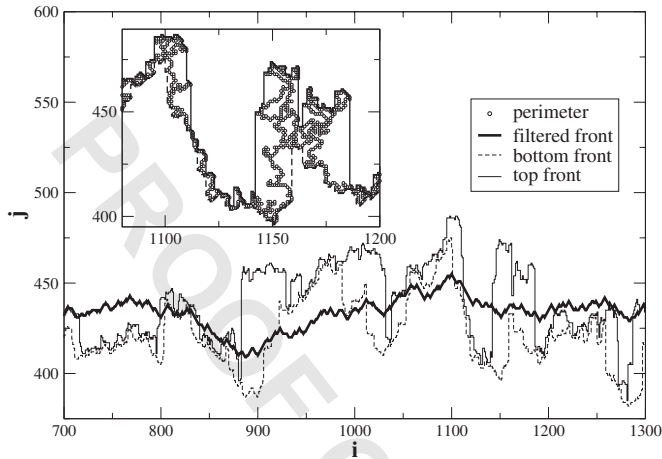


FIG. 1. Top-side and bottom-side SOS fronts based on the perimeter of the cluster connected to the  $p=1$  edge (shown in the inset as dots). We also show the filtered  $j_0(i)$  front [see Eq. (6)].

ponent  $\zeta=1/\beta$ . However, in this example, satisfying Eq. (1) is due to the step size distribution and not to spatial correlations [15,16].

We have used the average wavelet coefficient (AWC) method [17,18] to analyze the structure of the SOS fronts. The AWC method consists of wavelet transforming  $j(i)$ , and averaging the wavelet coefficients  $w(b,a)$  at each length scale  $a$  over position  $b$ ,  $W(a)=\langle w(b,a) \rangle_b$ . If  $j(i)$  is self-affine, the averaged wavelet coefficients will scale as

$$W(a) \sim a^{\zeta+1/2}. \quad (2)$$

We show in Fig. 2, the averaged wavelet coefficients based on the Daubechies-4 wavelets for the bottom-side fronts. The plots for the top and average fronts are comparable. The data are based on averages over 2201 samples for  $L_j$  in the range 64–2048 and 200 samples for  $L_j=4096$  and 8192.  $L_i$  was set

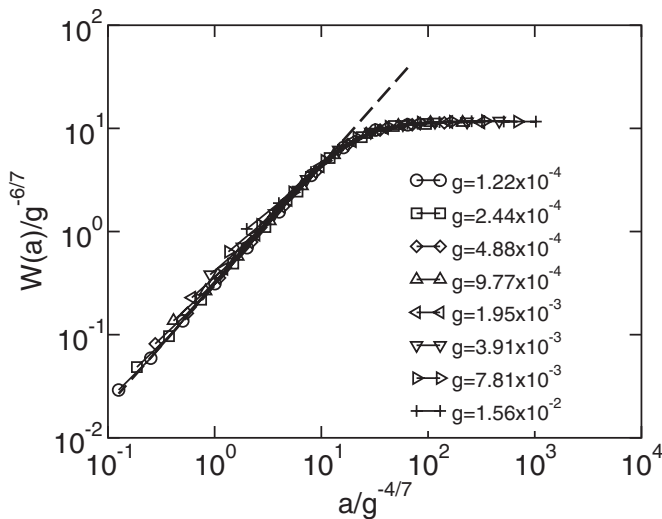


FIG. 2. Data collapse of the averaged wavelet coefficients for the bottom side front based on lattice size  $L_j=64$  to 8192, while  $L_i=2048$ . We show that  $g=1/L_j$ . The straight line has a slope of  $\zeta+1/2$ , [see Eq. (2)].

to 2048 for all the different  $L_j$ . The gradient  $g$  was set to  $1/L_j$ . There is a clear crossover between two regimes in these plots. At smaller length scales, one does indeed find the behavior of Eq. (2) indicating self-affinity. On larger scales, the slope of the log-log plots are zero indicating  $\zeta=-1/2$ , which corresponds to uncorrelated or white noise [19]. Furthermore, we observe excellent data collapse when  $W$  is scaled by  $g^{-\beta}$  and the length scale  $a$  is scaled by  $g^{-\alpha}$ . We will show below that

$$\zeta = 2 - D_e = \frac{2}{3}, \quad (3)$$

$$\alpha = \frac{\nu}{1+\nu} = \frac{4}{7}, \quad (4)$$

and

$$\beta = \frac{3}{2}\alpha = \frac{6}{7}, \quad (5)$$

where  $D_e=4/3$  is the fractal dimension of the external perimeter of the front [21].

The main goal of this Rapid communication is to derive Eq. (3) and thus demonstrate that  $\zeta$  is a proper Hurst exponent and  $j(i)$  is a self-affine function. To this end, we need to demonstrate two things: First,  $j(i)$  satisfies the scaling relation (1) and, second, that this is not due to a power-law tail in the step size distribution. We note that since the average wavelet coefficients obey Eq. (2),  $j(i)$  automatically satisfies Eq. (1). Therefore, we now need only to identify the mechanism behind this scaling.

In order to derive Eq. (3), we start by noting that the distribution of distances  $m$  between crossing points between a planar fractal curve with dimension  $D_e$ —e.g., the percolation perimeter—and a straight line follows the power-law  $\pi(m) \sim m^{-D_e}$  [20]. Introducing a gradient in the  $j$  direction and placing the straight line in the critical region interval  $[j_-, j_+]$ , and parallel to the  $i$  axis, the distribution of crossing point distances  $m$  remains the same. A self-affine curve characterized by a Hurst exponent  $\zeta$ , leads to a distribution of crossing point distances given by  $\pi(m) \sim m^{-(2-\zeta)}$  [20]. By comparing this expression to  $\pi(m) \sim m^{-D_e}$ , Eq. (3) immediately follows. However, we still need to show that  $j(i)$  is indeed self-affine, in other words the scaling relation Eq. (1) is not caused by jumps.

First, we turn to deriving Eqs. (4) and (5). The correlation length in the direction of the gradient, the  $j$  direction, is  $\xi \sim g^{-\nu/(1+\nu)}$ . Since the perimeter is locally isotropic, this is also the correlation length in the  $i$  direction. The crossover length scale from self-affinity to uncorrelated noise is the correlation length  $\xi$ . Hence, rescaling  $a \rightarrow a/\xi \sim a/g^{-\nu/(1+\nu)}$  gives data collapse along this axis, which demonstrates Eq. (4). Likewise, the crossover length scale in the  $j$  direction is  $\xi$ . This implies that the normalized wavelet coefficient at this scale,  $W(\xi)/\xi^{1/2}$ , is equal to  $\xi$ . Hence,  $W(\xi) \sim \xi^{3/2} \sim g^{-(3/2)\alpha} \sim g^{-\beta}$ , and  $\beta=(3/2)\alpha=6/7$ , as stated in Eq. (5).

In order to show that  $j(i)$  is a self-affine function, we need to demonstrate that  $\zeta$  is not caused by the step size distribu-

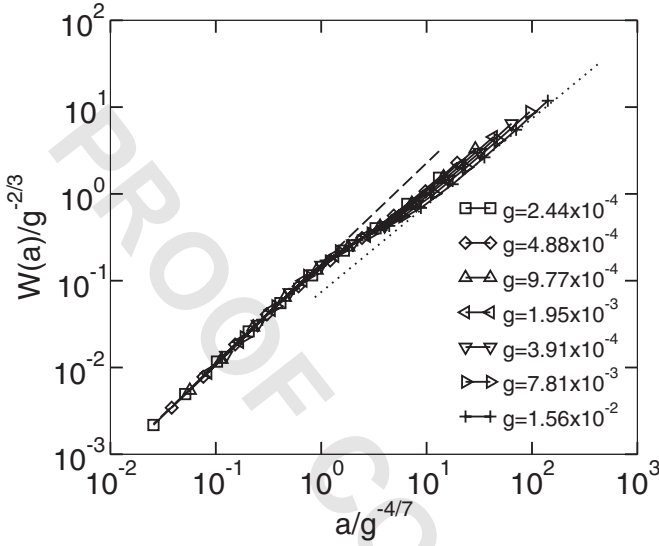


FIG. 3. Data collapse of the averaged wavelet coefficients for the smoothed  $j_0(i)$  based on the bottom side front. The lattice sizes and gradients are as in Fig. 2. The long-dashed line has a slope of  $7/6$  [see Eq. (2)], whereas the dotted line has a slope of  $1=1/2+1/2$ , consistent with uncorrelated random walks.

tion. To this end, we define the following transformation of the function  $j(i) \rightarrow j_k(i)$ , where we factorize the function in such a way that we can distinguish the respective roles of persistency and step sizes,

$$j_k(i) = \sum_{m=0}^i \text{sgn}[j(m+1) - j(m)] |j(m+1) - j(m)|^k, \quad (6)$$

where  $|j(m+1) - j(m)| = h(m)$  is the step size at position  $m$ . We have, in particular, that  $j_1(i) = j(i)$ . It was shown in [11] that  $h$  is distributed according to

$$N(h, g) = h^{-D_e-1} f(hg^\alpha), \quad (7)$$

where  $D_e = 4/3$  and  $f(z)$  approaches a constant as  $z \ll 1$  and falls off faster than any power law as  $z \rightarrow \infty$ . The step size distribution comes from the appearance of overhangs in the perimeter. An overhang is defined as the jump made by the front from one position along the  $i$  axis to the next due to a backwards turn [11,13,14]. In order to confirm that the overhangs do not generate the Hurst exponent  $\zeta = 2/3$ , we analyze the filtered front  $j_0(i)$ , defined in Eq. (6). With  $k=0$ , we eliminate the overhangs altogether [22]. Figure 3 shows the data collapse based on  $j_0(i)$  corresponding to the bottom side  $j(i)$  shown in Fig. 2. The scaling along the  $i$  axis is unchanged as no change in the system has been made in that direction. However, since all step sizes have been reset to unity in the transformation  $j(i) \rightarrow j_0(i)$ , the rescaling in the  $j$  direction is no longer controlled by  $j_c$ . In order to regain data collapse for different  $g = 1/L_j$ , we need to rescale the lattice units in this direction by the Hurst exponent  $\zeta = 2/3$ . The straight line matching the small- $a$  region of the figure has a slope  $2/3+1/2$ , while the straight line matching the large- $a$  portion has a slope of  $1/2+1/2$  corresponding to an uncorrelated random walk. This shows that, for small scales, the

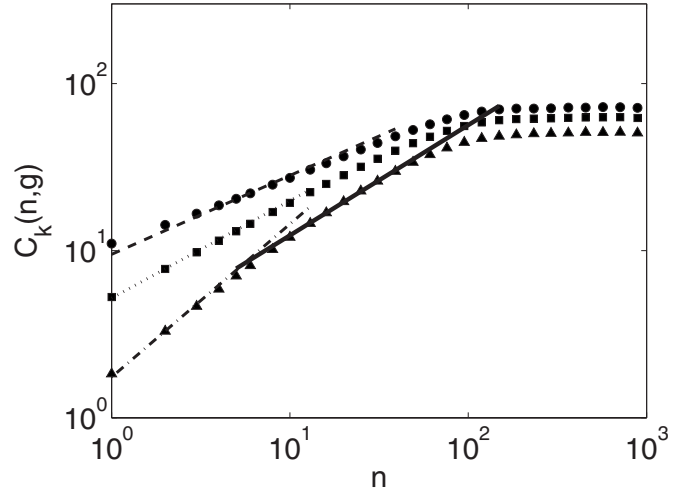


FIG. 4.  $C_k(n, g)$  as a function of  $n$  for  $k=1, 2$ , and  $3$ . The three leftmost straight lines have slopes according to Eq. (8), while the bold middle line has a slope equal to  $2/3$  in accordance with Eq. (9). For large  $n$  the structure functions become flat indicating that one has reached the decorrelated regime.

$\zeta = 2/3$  is indeed a Hurst exponent. On the other hand, for longer length scales, we expect random walk behavior since white noise gives precisely the exponent  $1/2$  in the transformation  $j(i) \rightarrow j_0(i)$ .

In order to analyze the multifractality that has been reported in this problem [12], we construct the structure function  $C_k(n, g) = \langle |j(m+n) - j(m)|^k \rangle$ . Multifractality occurs when  $C_k(n, g)^{1/k}$  does not scale with a single  $k$ -independent exponent with respect to  $n$ . Using the overhang distribution (7), we find  $C_k(1, g) \sim g^{s(k)}$ , where  $s(k) = \min[0, \alpha(D_e - k)] = \min[0, (16/21 - 4k/7)]$ . The self-affine character of  $j(i)$  cannot be visible in the structure function for  $n=1$  but will appear only gradually as  $n$  is increased. We may therefore analyze the structure function based solely on the Lévy character induced by the overhangs in the small- $n$  limit. We will call this the Lévy regime, whereas for larger  $n$ , where the self-affinity dominates, we will refer to it as the self-affine regime. The scaling with respect to  $g$  for  $C_k(1, g)$  persists for  $n > 1$  in the Lévy regime since  $j(i+n) - j(i)$  follows a Lévy distribution whose power-law tail does not change with increasing  $n$ . Hence, we expect  $C_k(n, g) \sim g^{s(k)}$  in this regime. In order to derive its dependence on  $n$  in the Lévy regime, we note that the distribution of distances  $l$  between overhangs follows the same power law as the overhangs themselves. This can be seen as follows. When there is a gradient present in the  $j$  direction, the length of the perimeter scales as  $L_i^{D_e}$ , when the gradient is kept fixed. Making a cut through the perimeter with a straight line parallel to the  $i$  axis, the crossing points of the perimeter with the line form a fractal set with dimension  $D_e - 1$ . Hence, there are, in a given interval  $l$ ,  $N_l \sim l^{D_e-1}$  overhangs [20]. These overhangs give rise to an effective Hurst exponent  $1/D_e = 3/4$  on the fractal set, seen, e.g., in the width of the trace,  $\Delta j \sim N_l^{1/D_e} \sim l^{(D_e-1)/D_e}$ . Since the overhangs form a fractal set, we will need  $N_b \sim l^{-(D_e-1)}$  boxes of size  $l$  to cover it. Due to the averaging over position  $i$ , there will be yet another factor  $l$  (see [23]).

We may now assemble these pieces to form the scaling of the structure function in the Lévy regime,  $C_k(l, g) \sim N_l^k N_b l \sim l^{k\zeta_k^L}$ , where

$$\zeta_k^L = \left[ 1 - \frac{1}{D_e} \right] + \frac{2 - D_e}{k} = \frac{1}{4} + \frac{2}{3k}. \quad (8)$$

Therefore, in the Lévy regime, i.e., for small  $n$ , there is multiaffinity. A similar analysis in the self-affine regime, i.e., at larger  $n$ , yields

$$\zeta_k^{SA} = \zeta = \frac{2}{3}. \quad (9)$$

Therefore there is no multiaffinity in this regime. The  $n$  for which there is the crossover between the Lévy and the self-affine regime will depend on  $k$  and is governed by the prefactors that the scaling analysis presented here cannot access. For  $n$  beyond  $\xi$ , the front decorrelates and the structure function becomes independent of  $n$ . We show in Fig. 4 the  $k=1$ , 2, and 3 structure functions. Their behavior is in accordance with our predictions. However, note that for  $k=2$ ,  $\zeta_2^L=7/12$

$=0.58$ , which is close to  $\zeta=2/3$ . Furthermore, the self-affine regime is close to the decorrelated flat regime. Hence, it is hard to distinguish between the Lévy and the self-affine regime for this value of  $k$ . As  $k$  increases, the Lévy regime grows, as the overhangs are emphasized for larger  $k$ .

To conclude, we have shown that the structure of the interface in a gradient percolation problem combines fractal and self-affine properties. The perimeter that includes numerous overhangs has the classical fractal structure [10]. However, solid-on-solid fronts that are extracted from the perimeter, have a clear self-affine property up to a crossover length scale  $\xi$  even if local jumps, inherited from overhangs, are removed. On larger scales it shows an uncorrelated noise behavior. The structure function is, however, sensitive to the overhangs on smaller scales and this implies a multiaffine scaling behavior in this regime. Implications of our results for physical interpretations of analogical and numerical experiments are important.

We thank M. K. Alava and S. Zapperi for stimulating comments leading to this work. G.G.B. thanks NTNU and Norsk Hydro.

- 
- [1] E. Bouchaud, J. Phys.: Condens. Matter **9**, 4319 (1997); **55**, 349 (2006).
- [2] B. B. Mandelbrot, D. E. Passoja, and A. J. Paullay, Nature (London) **308**, 721 (1984); S. R. Brown and C. H. Scholz, J. Geophys. Res. **90**, 12575 (1985).
- [3] E. Bouchaud, G. Lapasset, and J. Planés, Europhys. Lett. **13**, 73 (1990); K. J. Måløy, A. Hansen, E. L. Hinrichsen, and S. Roux, Phys. Rev. Lett. **68**, 213 (1992).
- [4] M. Cieplak and M. O. Robbins, Phys. Rev. Lett. **60**, 2042 (1988); M. Cieplak and M. O. Robbins, Phys. Rev. B **41**, 11508 (1990); N. Martys, M. O. Robbins, and M. Cieplak, *ibid.* **44**, 12294 (1991); H. Ji and M. O. Robbins, *ibid.* **46**, 14519 (1992).
- [5] G. Drazer, H. Auradou, J. Koplik, and J. P. Hulin, Phys. Rev. Lett. **92**, 014501 (2004).
- [6] A. Hansen and J. Schmittbuhl, Phys. Rev. Lett. **90**, 045504 (2003); J. Schmittbuhl, A. Hansen, and G. G. Batrouni, *ibid.* **90**, 045505 (2003).
- [7] M. J. Alava and S. Zapperi, Phys. Rev. Lett. **92**, 049601 (2004); J. Schmittbuhl, A. Hansen, and G. G. Batrouni, *ibid.* **92**, 049602 (2004).
- [8] J. Schmittbuhl, F. Schmitt, and C. Scholz, J. Geophys. Res. **100**, 5953 (1995); E. Bouchbinder, I. Procaccia, S. Santucci, and L. Vanel, Phys. Rev. Lett. **96**, 055509 (2006).
- [9] S. Santucci, J. Mathiesen, K. J. Måløy, A. Hansen, J. Schmittbuhl, L. Vanel, A. Delaplace, J. Ø. H. Bakke, and P. Ray, e-print cond-mat/0607385.
- [10] B. Sapoval, M. Rosso, and J. F. Gouyet, J. Phys. (France) Lett. **46**, L149 (1985).
- [11] L. Furuberg, A. Hansen, E. L. Hinrichsen, J. Feder, and T. Jøssang, Phys. Scr., T **38**, 91 (1991).
- [12] J. Asikainen, S. Majaniemi, M. Dubé, and T. Ala-Nissilä, Phys. Rev. E **65**, 052104 (2002).
- [13] A. Hansen, T. Aukrust, J. M. Houlik, and I. Webman, J. Phys. A **23**, L145 (1990).
- [14] G. G. Batrouni and A. Hansen, J. Phys. A **25**, L1059 (1992).
- [15] A. Hansen and J. Mathiesen, in *Modelling Critical and Catastrophic Phenomena in Geoscience: A Statistical Physics Approach*, edited by P. Bhattacharyya and B. K. Chakrabarti (Springer Verlag, Berlin, 2006).
- [16] J. Schmittbuhl, A. Hansen, and G. G. Batrouni, Phys. Rev. Lett. **90**, 045505 (2003).
- [17] A. R. Mehrabi, H. Rassamdana, and M. Sahimi, Phys. Rev. E **56**, 712 (1997).
- [18] I. Simonsen, A. Hansen, and O. M. Nes, Phys. Rev. E **58**, 2779 (1998).
- [19] A. Hansen, J. Schmittbuhl, and G. G. Batrouni, Phys. Rev. E **63**, 062102 (2001).
- [20] A. Hansen, K. J. Måløy, and T. Engøy, Fractals **2**, 527 (1994).
- [21] T. Grossmann and A. Aharony, J. Phys. A **19**, L745 (1986); T. Grossmann and A. Aharony, *ibid.* **20**, L1193 (1987).
- [22] G. M. Buendía, S. J. Mitchell, and P. A. Rikvold, Microelectron. J. **36**, 913 (2005).
- [23] S. J. Mitchell, Phys. Rev. E **72**, 065103(R) (2005).